Landscape Ecology **15:** 407–423, 2000.

Fire-driven dynamic mosaics in the Great Victoria Desert, Australia

II. A spatial and temporal landscape model

Daniel T. Haydon[1,*], John K. Friar[2] & Eric R. Pianka

Department of Zoology, University of Texas at Austin, Austin, Texas 78712-1064, USA; [1]*Corresponding author: Centre for Tropical Veterinary Medicine, Easter Bush, Roslin, Midlothian, Scotland EH25 9RG;* [2]*Current address: 'Widbrook', Wyatts Green Lane, Brentwood, Essex, UK CM15 0PY*

*(*author for correspondence, e-mail: Daniel.Haydon@ed.ac.uk)*

Received 25 August 1998; Revised 10 May 1999; Accepted 10 July 1999

Key words: Great Victoria Desert, habitat mosaics, intermediate disturbance, landscape processes, patch dynamics, singular value decomposition, spatial correlation, succession, time series analysis, wild fires

Abstract

An explicitly spatial, large scale, high resolution model of fire driven landscape dynamics in the Great Victoria Desert is constructed and parameterized to simulate frequency distributions of fire size and shape obtained from previous analyses of satellite chronosequences. We conclude that probabilities of fire spread cannot be constant over time, and that realistic distributions of fire size and plausible rates of fire spread can be obtained by assuming that fire spread is conditional on observed durations of windy conditions. Landscapes subject to this form of disturbance show large scale correlation structure many times greater than the average dimensions of single fires, and exhibit low frequency quasi-periodic stochastically driven oscillations in proportions of the landscape at different successional states over spatial scales exceeding 100,000 km^2. Average fire return intervals are ~30 yrs. Analysis of patch structure suggests that this landscape is composed of few large younger patches, embedded in a mature sea of surrounding habitat. Intermediate and late successional habitat must exist in more abundant patches somewhat smaller than young habitat. Numerous small patches of mature habitat are likely to be scattered throughout this younger habitat. The model predicts that fire size frequency distributions are relatively insensitive to changes of as much as ±50% of observed fire ignition frequency.

Introduction

The intermediate disturbance hypothesis is a central tenet of ecosystem ecology that predicts that highest levels of species diversity will be encountered at intermediate levels of ecosystem disturbance (Huston 1996). Many potential agents of disturbance can act across a wide range of spatial scales in many different guises (Pickett and White 1985). Wildfires are an agent of disturbance operating at some of the largest scales and are responsible for structuring many vegetated ecosystems. Fire resets successional cycles and maintains vegetative structural and taxonomic diversity within ecosystems, thereby facilitating coexistence of diverse fauna composed of species characteristic of different seral stages (e.g., Taylor 1973; Romme 1982). Temporal and spatial extent of wildfires in landscapes results from a complicated and poorly understood interaction of rates of fuel accumulation, frequency of ignition events, and factors controlling fires spreading across landscapes (Griffin et al. 1983; Johnson 1991; Iwasa and Kubo 1995; Boychuk et al. 1997; Li et al. 1997). These factors combine to determine static and dynamic characteristics of habitat mosaics that form over landscapes (Pickett and White 1985; Hansson et al. 1995).

As ecologists come to better understand the role of space and spatial heterogeneity in determining species population ecology, it is becoming clear that the spatial correlation structure of disturbance agents has important impacts on distribution, abundance and persistence times of species inhabiting heterogeneous landscapes (e.g., Paine and Levin 1981; Hansson et al.

1995; Lindenmayer and Possingham 1995; Moloney and Levin 1996; Li and Apps 1996). Due to the antiquity of interplay between landscape and fire, species autecologies have probably evolved in direct response to such large scale disturbance (Pianka 1996). Developing an understanding of the evolutionary ecology of these species assemblages is one reason to study dynamics of fire driven mosaics. Another, more pressing motivation is that an understanding of landscape dynamics at their largest scales is urgently required to formulate conservation plans sufficient to effectively preserve species assemblages in habitat mosaics. Anthropogenic influences on fire driven ecosystems are numerous, and include fuel harvesting (timber extraction, grazing, etc., see for example, Wallin et al. 1996; Schimmel and Granstrom 1997; Russellsmith et al. 1997), habitat conversion and fragmentation (through agricultural sequestration or urbanization, see, for example Morton et al. 1995; Gill and Williams 1996), introduction of fire management (through active fire suppression or increased frequency of ignition, see, for example, Baker 1993, 1994; Minnich and Chou 1997; Russellsmith et al. 1997) and consequences of climate change (e.g., Gardner et al. 1996). All these influences could have possibly profound effects on characteristics of dynamic habitat mosaics that have arisen through the long interaction of fire with the landscape.

To date, detailed, long term, large scale, quantitative models of fire driven landscape dynamics (as distinct from highly tactical models predicting likely spread of single fires) have been mostly undertaken for forested systems (e.g., Green 1989; Baker et al. 1991; Antonovski et al. 1992; Ratz 1995; Li et al. 1997; Boychuk et al. 1997). However, the Florida everglades (Wu et al. 1996) and Australian and South African heathland systems (Bradstock et al. 1996) have also received attention. Methodological scaling problems with explicit modelling of long term, large scale spatial processes are well established (Mckenzie et al. 1996) but only recently have sufficiently powerful computers been generally available to run models at spatial resolutions at which such scale problems can be reduced. Here we exploit this computational power to develop a mechanistic, wind driven fire simulation model run at high resolution (80 m $\times$ 80 m) over landscapes exceeding a 100,000 km^2. Increased availability of satellite imagery plus reduced costs of computer hardware and software required for development and analysis of these numerically intensive models should soon render such analyses more common.

We use the model to attempt to improve current understanding of the role of fire on landscape dynamics of spinifex grasslands in the Great Victoria Desert of Western Australia. Basic features and previous studies of this ecosystem are summarized in the introduction to the preceding paper (Haydon et al. 1999). Average fire size in the GVD is approximately 28 km^2, with a maximum of 5% of the landscape burning every year (Haydon et al., 1999). We exploit the description of real fires undertaken in the preceding paper to construct and fit a large scale simulation model of landscape dynamics to understand and predict possible landscape patterns that will arise from existing and possible alternative fire management practices. Specifically, we are interested in what modelling exercises suggest about the way fires currently burn and particularly what limits their spread. Model parameters are selected that result in simulated landscapes with attributes closely approximating those deduced from corresponding satellite imagery of the region (Haydon et al. 1999). Using these parameter values, model output allows us to predict various structural and dynamic characteristics of real landscapes that are not measurable directly from imagery, these include: pixel age structure, patch age/size structure and spatial correlation structure. We predict changes in landscape characteristics that would result from adoption of different fire management strategies.

The model

Our previous study (Haydon et al. 1999) suggested that 5% is an upper estimate for the average fraction of hummock grassland that burns each year. Vegetation recovers quickly following fire, and reburn in similar substrates in the central ranges has been reported to be possible within 3–10 years (Kimber 1983) suggesting that at any point in time a large fraction of the landscape is potentially burnable. Furthermore, fire disturbance is clearly a highly autocorrelated process, and it is unlikely that these unburnable fire scars could be distributed in a manner that does not leave the remaining landscape largely contiguous. Theoretical studies of wildfire and epidemiological processes have determined that spread of fire or disease through largely homogenous 'substrates' is governed by a critical transmission threshold, above this threshold, fire or disease spreads on a very large scale, below this threshold the probability of substantial spread is negligibly small (e.g., Isham 1991; O'Neill et al. 1992).

Only two general mechanisms permit spatially contagious disturbance over intermediate scales. The first is to restrict attention to very narrowly defined regions around the transmission threshold, the second is to introduce some spatial or temporal heterogeneity to the transmission process (as suggested by Turner et al. 1994a). Here we argue against this first possibility and for the second, for the following reasons:

(1) Analytic models of the spread of contagious disturbance over homogenous substrates at around critical transmission rates predict that the probability density function of final disturbance size should be a reflected 'J' shape (Kendall 1956), i.e., one that is monotonically decreasing. This is not the shape of density functions for observed fire sizes (Haydon et al. 1999).

(2) Simulation models and percolation theory relating to spread of contagious disturbance over homogenous substrates at around critical transmission rates predict that the disturbance is very 'porous', that many small islands and 'fjords' are left unburnt within the surrounding circumference of the fire (e.g., Stauffer and Aharony 1992). But our preceding analysis of fires in this region reveals that real fires are 97% 'solid', with only 3% of the area enclosed by the external perimeter remaining unburnt (Haydon et al. 1999). Such solidity is consistent with transmission rates much higher than 'close to critical'. Put more intuitively, if transmission rates are high enough that fires burn over 97% of their enclosed area, then why would they ever stop burning before spreading over the remainder of the landscape? Under such circumstances, how could over 50% of potentially burnable landscape escape fire each year? The same arguments suggest that the reasons fires burn out have more to do with temporal than with spatial heterogeneity, and lead us to suggest that wind is the most likely agent of temporal heterogeneity in rates of spread. This is supported by two additional lines of evidence:

(3) In experimental burns on similar substrates, wind speed is clearly related to fire size and speed of spread (Burrows et al. 1991; Bradstock and Gill 1993, Griffin and Allan 1984).

(4) The influence of prevailing wind direction is clearly discernible in shapes of fire scars analyzed in the preceding paper (Haydon et al. 1999).

We develop a simulation model of fire dynamics in which fire spread is assumed to be contingent on wind strength. We do not claim that spatial distribution of permanently unburnable landscape features does not influence fire size and shape, only that landscape dynamics in this system can be reasonably approximated for large homogenous regions without explicitly accounting for unburnables.

Analysis of wind data

Information on wind strength and direction was acquired from the Australian Meteorological Bureau in Perth. These data were collected at Yamarna weather station located near the center of the imagery. Wind data collected at 5 m above ground level were available at two times (0900,1500) each day and spanned 19 years (1977 through 1996). Wind strength was classified in to one of five categories (< 2 m/s, $\geq 2 < 5$ m/s, $\geq 5 < 8$ m/s, $\geq 8 < 11$ m/s, ≥ 11 m/s). From these data we calculated (1) the probability that wind would blow at a particular strength at 1500 on any given day; and (2) two transition matrices governing the probability that it would blow at a particular strength at either 0900/1500 given that it had blown at specified strength at the last time of recording (1500/0900). These matrices are reported in Appendix 1. There was no marked seasonality in these probabilities. Wind direction was classified as blowing in one of eight directions (see Haydon et al. 1999), and corresponding probabilities of wind direction calculated. Data indicated that over the duration of a period during which wind speed exceeded 5 m/s direction was fairly stable, with less than a 15% probability of exceeding a 45° change from its last recorded direction. Figure 1A shows the probability distribution of duration of wind episodes (defined as the time interval from when wind speed first exceeded 5 m/s to when it dropped below 2 m/s) deduced from real data, and from modelling wind episodes with the two transition matrices. Agreement is good, distributions are (not surprisingly) close to exponential, with means of ~2.7 days.

Description of fire model

The landscape was modelled as a flat two dimensional $n \times n$ (n between 1500 and 4000) rectangular lattice of pixels with absorbing boundary conditions. To render simulation results directly comparable with analysis of satellite imagery, simulations were conducted at the same spatial resolution as the imagery (1 pixel equivalent to an area 80 m $\times$ 80 m). Time (in years) since fire last burned over a pixel is recorded and referred to as the pixel's 'age'. Pixels either burn or not, and all pixels recover from fire at the same rate, thus we ignore possible recovery rate heterogeneities that might arise from variations in fire intensity, overall fire size

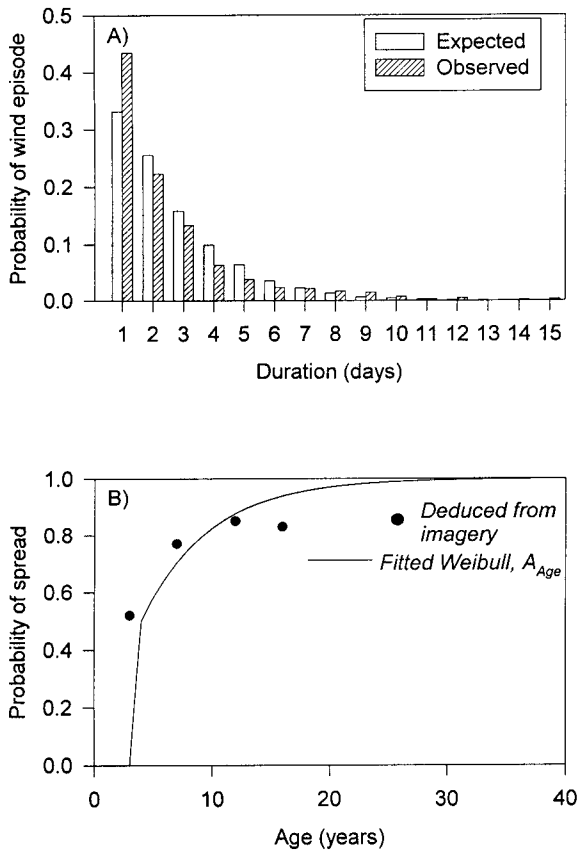

Figure 1. (A) Probability distribution of duration of wind episodes (defined as the time interval from when wind speed first exceeded 5 m/s to when it dropped below 2 m/s) deduced from wind data (hatched bars), and from modelling wind episodes with two transition matrices (unhatched bars). Agreement is good, distributions are close to exponential, with means of ~2.7 days. (B) Probability of fire spread via secondary ignition events. Solid circles are empirical estimates of probability of fire spread obtained from satellite imagery data (see Haydon et al. 1999), solid line shows fitted Weibull function (A_{age}, truncated to zero for pixels 3 years or less).

(factors that have been shown to be important in other systems, e.g., Turner et al. 1994b, 1997) and rainfall (Griffin et al. 1988).

The fire process is modelled with two types of ignition events (IEs). Fires start from a primary ignition event (1° IE), assumed to be a lightning strike, that results in the start of a fire involving a single pixel, chosen at random within the lattice. 1° IEs result in a fire over the selected pixel, regardless of pixel age. Fire spread to other pixels is determined by a sequence of secondary ignition events (2° IEs) described in detail in Appendix 2. The algorithm burns a number of fires each year specified by a random variable drawn from a Poisson distribution with mean equal to the observed mean intensity of fires obtained from the data (see Haydon et al. 1999), after which various structural attributes of the landscape are computed, and age of all pixels in the landscape incremented by 1 year.

The algorithm governing occurrence of fire spread through 2° IEs contains two crucial assumptions. First is that probability of fire spread to adjacent pixels is greater the longer the time interval since fire last burned over a pixel (this interval is referred to as pixel age). The exact relationship is shown in Figure 1B, and its computation fully described in Appendix 2. Fire probability increases rapidly with pixel age for pixels of age 3–8, after which the probability rises much more slowly. This is consistent with observed shortest fire return times (Kimber 1983) and the assumption that fuel loading is not strongly related to rates of fire spread (Burrows et al. 1991, but see Griffin and Allan 1984). The second assumption is that fire spread depends strongly on wind speed and does not occur at wind strengths below 2 m/s.

The computer program was written in Pascal using Borland Delphi, and run on 200 Mhz PCs with 128 megabytes of RAM. Landscapes of ~4 million pixels can be simulated for 200–400 years in about 12 hours. The program is available from DTH in various forms, on request.

Selection of model parameters

The landscape was initialized with random pixel ages selected uniformly between 1 and 255 years old, and the model iterated for 150 years prior to any data collection to allow transients to pass. At which point simulations were run for however long was required to burn a further 817 fires (the number of real fire scars recovered from imagery. – see Haydon et al. 1999). Area (A), perimeter (P), edge simplicity (ES) and ratio of major to minor axes (MM) are computed for each fire at the end of every year (fires that run together are treated as only a single fire). Frequency distributions for these geometric quantities for 817 simulated and the observed fires are then compared with a chi-squared statistic and an overall fit statistic (χ_0^2) calculated as: $\chi_0^2 = (\chi_A^2 + \chi_P^2 + \chi_{ES}^2 + \chi_{MM}^2)^{1/2}$.

Given the two major assumptions, the process of fire spread is essentially determined by 4 key parameters (see Appendix 2 for full details): (1) the number of trials available to each burning pixel prior to burning out, N; (2) the time interval represented by each of these trials, t; (3) the sensitivity of directional spread probabilities to wind strength, k_b; and (4) an overall

Table 1. Descriptive statistics of simulated fires for five variables (817 fires).

Statistic	Mean	SD	Min.	Max.
Area (km^2)	27.53	67.38	0.07	1098
Perimeter (km)	53.07	85.12	1.28	1266
Perimeter/Area	8.29	8.19	0.40	50.00
Major/minor	2.04	1.02	1.00	11.54
Edge simplicity index	0.108	0.07	0.006	0.589

tuning parameter that scales probability of any 2° IE, *F*. With these 4 parameters, a substantial degree of control was obtained over fire size, rate of spread, solidity, edge simplicity and shape.

Fitting models of this dimension and complexity and performing appropriate sensitivity analyses posed severe problems. We deliberately built some redundancy in to parameterization of this model, and by so doing have contained a large degree of the model's potential behavior within the parameter volume defined by 4 key parameters. The model was fitted to observed characteristics of real fires by tuning these 4 parameters. When data were unavailable for guiding estimation of other parameters, arbitrary values were used, but in these cases, the inbuilt redundancy permits this arbitrariness to be offset by having fitted a key parameter with which the unknown parameter was correlated (these points are discussed further in Appendix 2). We performed dozens of simulations using variously estimated combinations of these 4 parameters and arrived at a combination of parameter values that burned realistic populations of fires, which consistently yielded low values of χ_0^2. We then examined all 81 sets of parameter combinations formed by perturbing each of these 4 parameters by +30%, 0% or −30% of its optimum value in all possible combinations, to confirm that the estimated best overall fit represented at least a local minimum for χ_0^2.

Vital statistics of simulated fires are shown in Table 1, which should be compared with Table I in Haydon et al. (1999). Sensitivity analysis indicated that equally low values of χ_0^2 could be obtained by slightly different combinations of the 4 parameters (see Appendix 3). The estimated best overall fit to the four distributions yielded a χ_0^2 value of 523 (this set of parameters is henceforth called the 'control parameters'). Better fits could be obtained by fitting each distribution singly (lowest $\chi_A^2 = 105$, lowest $\chi_P^2 = 131$ lowest $\chi_{ES}^2 = 344$, and lowest $\chi_{MM}^2 = 105$). The model does not generate quite as many of the largest fires as observed in the imagery, and is deficient in some respect that results in simulated fires having greater average edge complexity than real fires. When the model is fitted only to the 3 observed distributions of area, perimeter and ratio of major:minor axes, χ_0^2 can be reduced to 230. Analysis of results from sensitivity analyses indicated that most individual χ^2 scores were either positively correlated or uncorrelated however χ_{ES}^2 and χ_{MM}^2 were negatively correlated, indicating that parameter combinations consistent with a good fit for one of these properties yielded a poorer fit with respect to the other.

Simulated fires were of approximately the same average area as observed fire scars and tended to contain within their perimeter a similar average percentage of unburned area to real fires (~3%). Selected control parameters limit the shortest time for fire to spread from one pixel to a neighboring pixel to $t = 9$ min, thus this parameter choice places an upper limit on the spread of a fire front of ~0.5 km/h. This rate is quite low compared to observed rates of head fire advance in experimental fires (Burrows et al. (1991) report a range of 0–5.5 km/h, (av. 1.12 km/h) for spinifex grasslands; while Cheney and Gould (1995) report 0.1–7.4 km/h in a different grassland fuel). However these empirical rates are averages measured over shorter durations and smaller fire fronts and may not be directly applicable to the lower spatial resolution and longer time frames addressed by our model.

Analysis of model landscapes

Model landscapes simulated using control parameters (referred to as control landscapes) were subjected to various analyses.

Pixel age distribution over the landscape

Figure 2 shows estimated cumulative probability density functions for pixel age determined at 10 year intervals for a century over a control landscape. The average age of a pixel is ~30 years. Between 4–12% of the landscape is between 0–4 years old, 14–31% is less than 12 years old, and between 34–47% up to 25 years old. Between 53–66% of the landscape is 26 years old or more. Pixel age distributions exhibit some temporal fluctuations indicating variation in exact landscape composition over time.

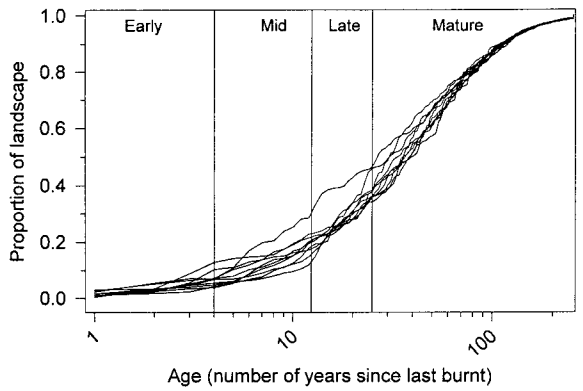

Figure 2. Cumulative age distribution of pixels in the landscape. Each line corresponds to the cumulative distribution of pixel ages in a control landscape of 4 million pixels (160 km on a side), recorded at 10 year intervals over 100 years. Note logarithmic x-axis (age classification is arbitrary, and purely for descriptive purposes).

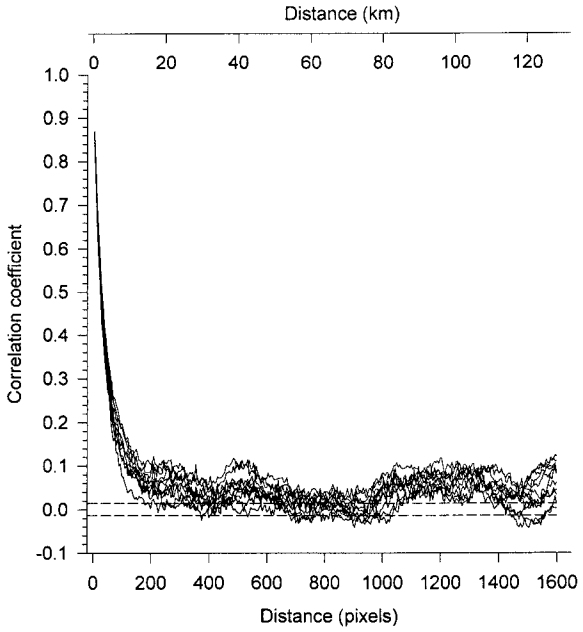

Figure 3. Spatial correlograms of pixel ages in control landscapes. Each line corresponds to the spatial correlogram of pixel ages in a control landscape of 4 million pixels (160 km on a side), recorded at 10 year intervals over 100 years. At each distance Moran's I statistic is calculated using 10,000 pairs of pixels. Dashed lines indicate two standard errors each side of the expected value of I in a fully uncorrelated landscape.

Perimeter area relationship

Perimeter and area of simulated fire scars was not quite as tightly correlated as observed fire scars ($r = 0.901$, compared to 0.986, Haydon et al. 1999) but was well described by the function $P = kA^g$. The constant g was higher than for observed fires (0.906, SD = 0.005, compared to 0.718, SD = 0.011). This difference was statistically significant, indicating that edge geometry of simulated fires was significantly more complex than those of real fires extracted from satellite imagery.

Correlation structure of the landscape

Two-dimensional spatial correlation of pixel ages determined at different scales within the landscape can be calculated using Moran's I statistic (see Davis 1993). Figure 3 shows a series of correlograms calculated for control landscape recorded at 10 year intervals over a period of 100 years. At distances of less than 200 pixels (~20 km) landscapes are strongly positively correlated, at greater distances of up to 800–1000 pixels (~75 km) there is some very weak positive correlation. However landscapes become more positively correlated at distances of 1200–1400 pixels (100–120 km). There is almost no evidence for substantial negative correlations within landscapes and no great temporal variation in correlation structure of landscapes.

Landscape mosaics arise from a combination of stochastic and deterministic processes. Location of 1° IEs and precise spatial sequence of 2° IEs are clearly partly stochastic processes. However, the aging process of vegetation and its increasing capacity to support 2° IEs through time are deterministic. The state of a single pixel over time is essentially purely stochastic and largely uninformative. For a sufficiently large area of landscape, a simple statistical average state over time is more deterministic and also uninformative of system dynamics. However, at some particular intermediate scale, the ratio of deterministic information to stochastic fluctuation is maximized. Methods have been developed that allow determination of this intermediate scale (Rand and Wilson 1995), but have yet to be applied to realistic landscape processes.

Define a sequence of square windows of dimension L pixels containing L^2 pixels ($L = 20, 40, 60 \ldots 4000$). Categorize pixels to be in one of 3 different classes: early successional (ages 0–4), mid-successional (ages 5–12) and late successional (age 13+). Record number of pixels, $X_{j,L}(T)$, in the jth ($j = 1 \ldots 3$) category in each L-window after each year (T) of fire activity over the landscape. Time series for L-windows of two different sizes illustrating proportions of each window in different successional categories are shown in Figure 4. Let $\sigma^2_{j,L}$ be the variance associated with $X_{j,L}(T)$. According to theory devel-

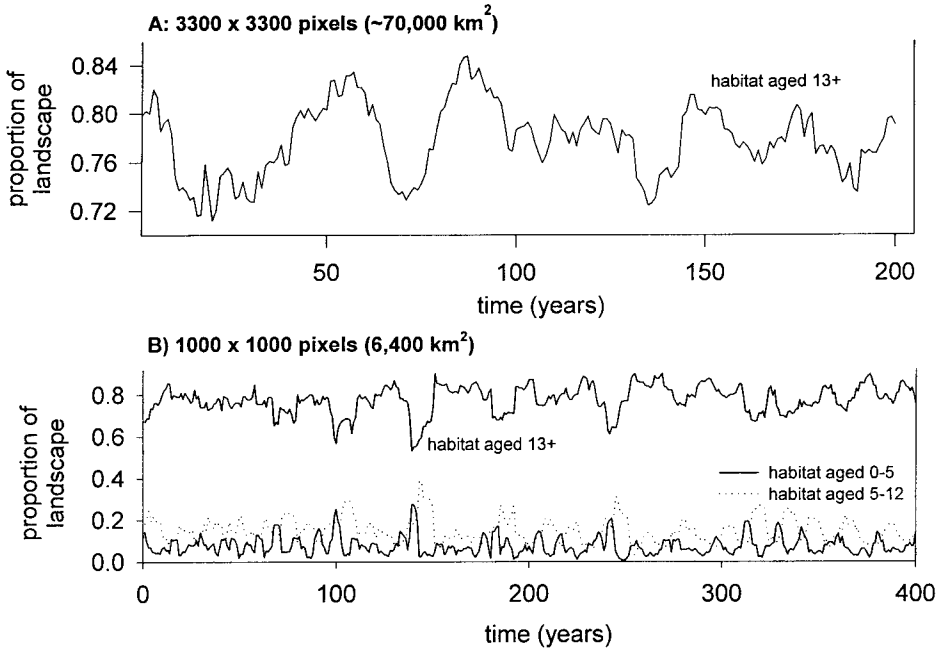

Figure 4. Time series of proportions of pixels in L-windows in different successional categories for control landscapes. (A) Habitat over 13 years old, $L = 3300$. (B) Habitat of different ages, $L = 1000$.

oped by Rand and Wilson (1995), peaks or asymptotes in plots of $\sigma^2_{j,L}/L^2$ against L should indicate the scale at which the ratio of deterministic information to stochastic fluctuation is maximized[1]. In essence this scale is a measure of the spatial 'size' of the dynamical process determining landscape structure.

Figure 5 plots $\sigma^2_{j,L}/L^2$ against L. This plot suggests that dynamics of early and mid-successional habitat are most informatively viewed in L-windows of between 1000–2000 pixels (80–160 km) in dimension. Dynamics of late successional habitat appear to extend to even larger spatial scales, possibly approaching as much as 100,000 km^2.

Time series analysis

Temporal variation in occurrence of different habitat types in windows of various sizes (see Figure 4) was subjected to spectral analysis (see Figure 6). All spectra suggested that habitat quantities experienced long wave length fluctuations. Mature habitat viewed at very large spatial scales (~11 million pixels, 70,000 km^2) showed a clear tendency of low amplitude cycling with periods of 200 and 30–50 years (Figure 6A). Computational constraints governing collection of long time series at this high spatial scale at these resolutions restricted further investigation of these cycles. At lower spatial scales (1 million pixels, 6400 km^2) habitat appeared to have cyclic components corresponding to frequency ranges that increased in breadth as age of habitat decreased. Mature habitat at these scales had cyclic components corresponding to periods of 200 and 25 years (Figure 6B), mid-successional habitat also exhibited a frequency peak corresponding to a 15 year cycle (Figure 6C) while early successional habitat cycled over a wider range of frequencies, including one with a pronounced 10 year period (Figure 6D).

We applied singular value decomposition (SVD) analysis to investigate dynamical properties of these time series Details of these methods are given by Broomhead and King (1986) and Abarbanel et al. (1993), and an example application is given by Rand and Wilson (1995). Briefly, the normalized time series is used to construct a sequence of row vectors $\overline{X}_{j,L}(T) = X_{j,L}(T - d + 1), X_{j,L}(T - d +$

[1]Another way of thinking about this theory is to imagine two L-windows immediately adjacent to each other, and record the number of pixels in each window over time. Clearly if L is small, then the same processes will likely affect the dynamics in both windows and a covariance will exist between the dynamics within each window. However as L is increased, a scale at which dynamics within each L window are independent of each other will be encountered. We are interested in determining the smallest value of L for which such independence exists.

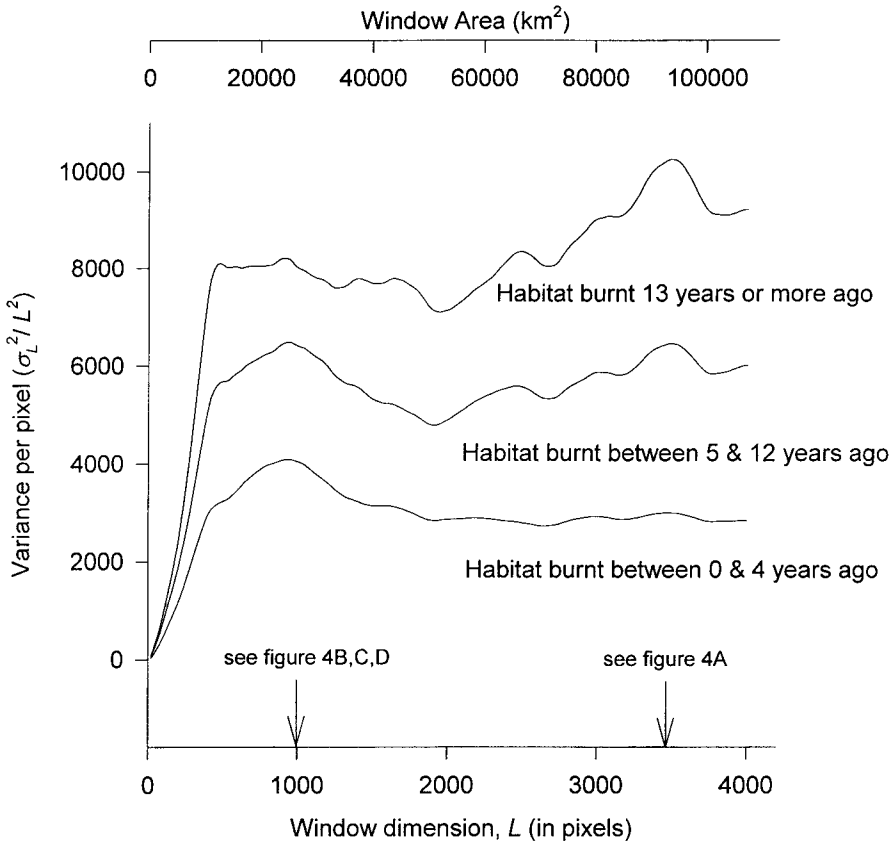

Figure 5. Scaling behavior of the modified variance $\sigma^2_{j,L}/L^2$ of time series in L-windows of different sizes for 3 different successional categories. Note peaks at $L \sim 1000$ pixels, and the larger scale peak at $L \sim 3300$. Arrows indicate spatial scales at which time series shown in figure 4 were sampled. Time series spanning 200 years were collected on control landscapes 4000 pixels on a side.

2), ..., $X_{j,L}(T)$, $T = d \ldots T_{\max}$, where $T_{\max}$ is the length of the time series. Parameter d is chosen to be large relative to dimensionality of underlying deterministic processes. Each $\overline{X}_{j,L}(T)$ vector is then used to form a row of a rectangular matrix $\mathbf{Y}$ termed the trajectory matrix. The SVD of this trajectory matrix is given by $\mathbf{Y} = \mathbf{S\Sigma C}'$, where $\mathbf{S}$ and $\mathbf{C}'$ are orthogonal matrices and Σ is a $d \times d$ diagonal matrix containing the singular (eigen)values. Interpretation of SVD is somewhat akin to principle components analysis, the idea is that some subset of d available dimensions will be occupied by any deterministic signal from the underlying process, (and indicated by singular values proportional in magnitude to the variation accounted for by those dimensions), and that remaining dimensions will be filled in some uniform manner by stochastic noise associated with the time series (and indicated by lower singular values). Thus inspection of singular spectra reveals both presence or absence of deterministic signal, and if present, its anticipated dimensionality.

Figure 7 shows singular spectra for 3 successional categories of habitat viewed within windows of 1000 pixels on a side. Dynamics of all age categories requires ~50 dimensions to capture the first 90% of variation in their time series. No single dimension accounts for more than 8% of the total variance in any of the time series. Overall SVD analysis suggests no evidence for any low dimensional deterministic signal in these dynamics, and that most likely they simply reflect fairly low frequency stochastic processes.

Patch size structure

Defining early, mid, late and mature successional habitat as pixels aged 0–4 yr, 5–12 yr, 13–25 yr and 26+ yr old, contiguous patches of landscape in the same successional state were identified. In a typical control landscape of 25,600 km^2 (160 km × 160 km),

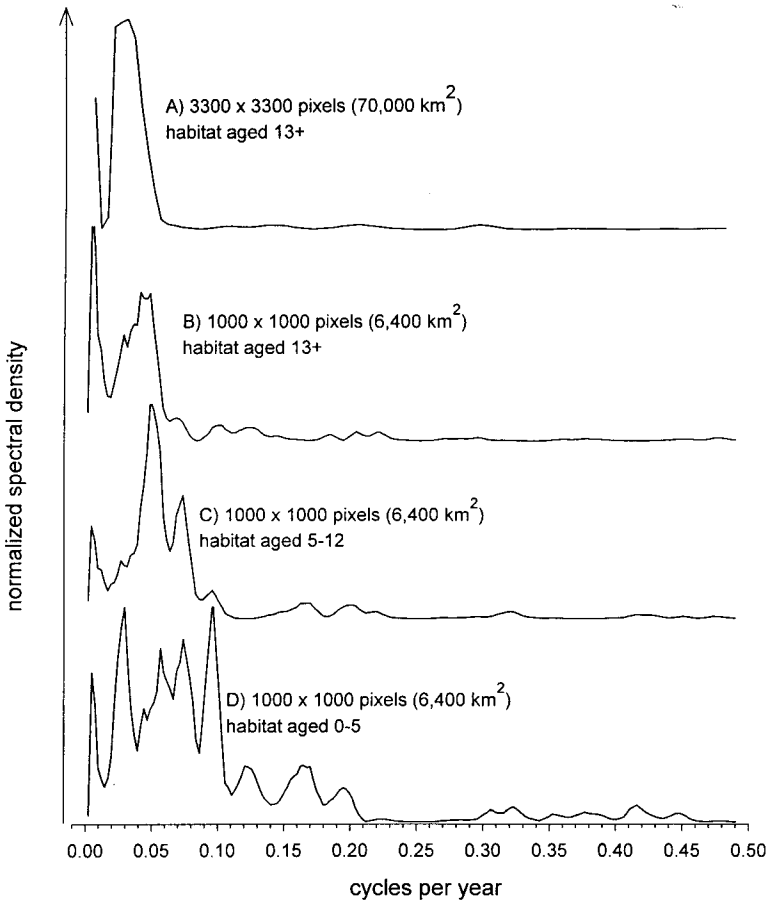

Figure 6. Results of spectral analysis applied to time series in Figure 4. Time series exhibited no identifiable trend, and were analyzed without any prior smoothing devices by applying a direct Fast Fourier Transform to raw data and smoothing coefficients. Very similar results were obtained by transforming the autocorrelation function (see Chatfield 1996). Time series are 406 years long (except A which is 200 years) with landscape composition sampled at the end of every year.

approximately 2/3 of land area is occupied by a single vast background patch of mature habitat. 80% of the remaining one third is accounted for by about 50 patches of various ages, the rest is fragmented into over 4000 much smaller patches. Average size of early and mid successional patches is ~15 km^2. Average size of late successional patches is about 6 km^2, mature patches are much smaller with an average size (omitting the dominant background patch) of 0.02 km^2 (see Table 3, row 3). While ~65% of the landscape is successionally mature by area, about 80% of landscape patches are mature ~20% of the landscape is late-successional by area, ~10% is mid-successional by area and ~5% early successional. Characteristic size frequency distributions of these patches are shown in Figure 8.

The overall picture is one of a largely mature landscape, into which are embedded relatively small numbers of younger successional patches. Nested with in these younger patches are numerous very tiny islands of mature habitat. Early and mid-succession patches are rare and quite large. Late successional patches are smaller and more numerous.

Interpatch distance analysis

Coordinates of the centroid of each patch in the landscape were calculated as the average coordinates of each pixel within that patch. Average distances between centroids of small to moderate sized patches represent patch connectivity. The same is not true of very large patches as distance between centroids and perimeters of very large patches may be large relative to the closest regions of the perimeters of two

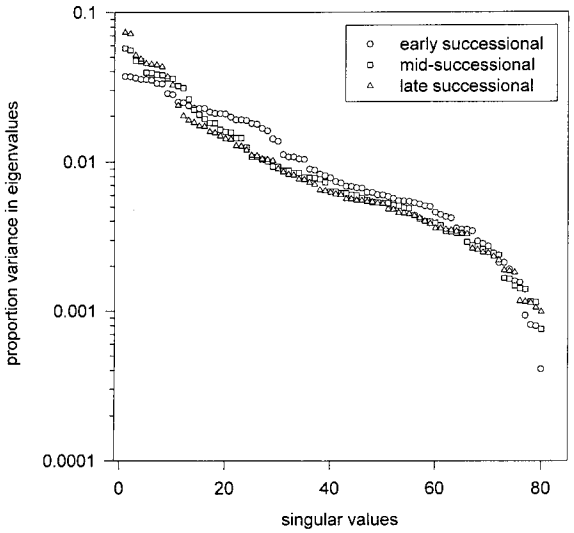

Figure 7. Singular spectra for times series shown in Figures 4B–D. $L = 1000$ pixels, $d = 80$, $T_{max} = 406$. The relatively even spread of variance over so many dimensions is consistent with the notion that time series are dominated by stochastic processes, and that low dimensionality determinism is absent. Time series were normalized to zero mean and unit standard deviation prior to analysis.

patches. Figure 9 shows average numbers of similarly aged patches found within circles of increasing radius centered on an average patch. Mid and late-successional patches are more densely scattered over the landscape relative to early successional patches. It is normally only necessary to travel about 0.5 km from one mid or late successional patch before encountering another, interpatch distance between early successional patches is approximately 12 km. Overall density of late successional patches is greater than mid- successional patches, but at distances of less than a kilometer from mid-successional patches one actually encounters more mid-successional patches than late-successional patches encountered within a kilometer of late-successional patches, indicating that at these scales, mid-successional patches are clumped. These findings may have important implications for patch specialized inhabitants.

Alternative ignition frequencies

We studied landscapes that arose from models in which rates of 1° IEs were decreased by up to 50%, and increased by as much as 150% over those of control landscapes. This tests sensitivity of our results to assumptions made about rates of 1° IEs, and it may indicate consequences of fire management strategies that result in fire suppression or proliferation. Average fire size is largely insensitive to changes of up to ±50% in frequency of 1° IEs, but does significantly decrease as this frequency is increased over 100% of control values (see Table 2). As a consequence of this behavior the average landscape age is proportional to the inverse of 1° IE frequency (Table 2). Cumulative frequency distributions of pixel age for landscapes simulated under these alternative fire regimes are indicated in Figure 10.

Table 2. Average fire size (with 1 standard error) and average pixel age in landscapes simulated with different rates of 1° IEs.

Fire regime	Average fire size (km^2) (standard error)	Average pixel age (yr)
1° IEs down 50%	33(2.9)	83
1° IEs down 25%	31(3.0)	53
Control	28(2.6)	50
1° IEs up 25%	32(2.7)	41
1° IEs up 50%	29(2.7)	35
1° IEs up 75%	26(2.4)	31
1° IEs up 100%	25(4.1)	30
1° IEs up 125%	24(3.0)	28
1° IEs up 150%	21(1.6)	25

As expected, landscape patch structure shifts toward a younger, patchier, more fragmented composition as fire frequency increases (see Table 3). Numbers of early, mid and late successional patches goes up (in contrast to the fraction of landscape that is mature), and their size goes down, but overall, percentage of landscape in younger successional stages increases markedly with 1° IE rates.

Discussion and conclusions

Development and analysis of this landscape model is instructive in several ways. First, combining information about average fire size, fire 'solidity', fire frequency and vegetation recovery time suggests that probabilities of fire spread from pixel to pixel (2° IE's) must ultimately decrease over time, particularly late in the life-time of the fire. In developing our simulation model we could not come close to realistic fire size distributions without imposing some form of temporal heterogeneity in probabilities of fire spread. We hypothesize that this heterogeneity is induced by variable wind conditions.

Rates of fire spread and the observed distribution of periods of windy conditions combine in a plausible

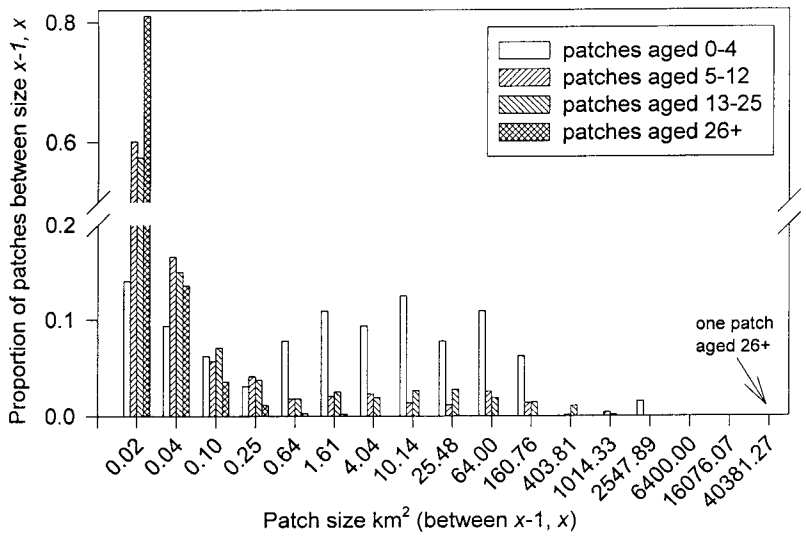

Figure 8. Size frequency distributions of patches of different successional stage deduced from one representative control landscape 160 km on a side. All proportions of patches of one successional stage sum to 1. One very large mature patch covering ~65% of the landscape is indicated in bottom right corner.

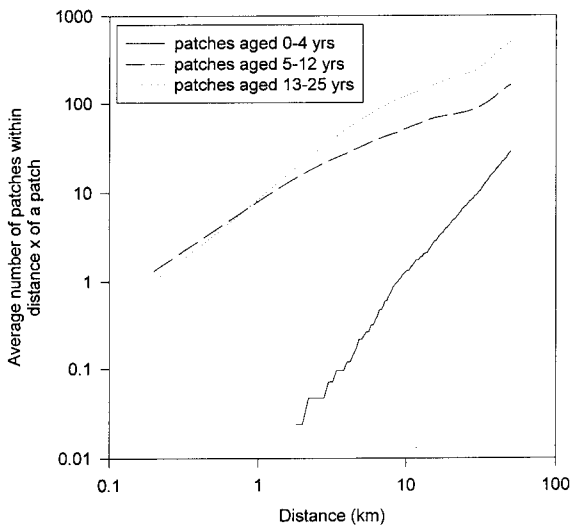

Figure 9. Average number of patches in same successional state (y-axis) within a specified radius (x-axis) of a given patch's centroid.

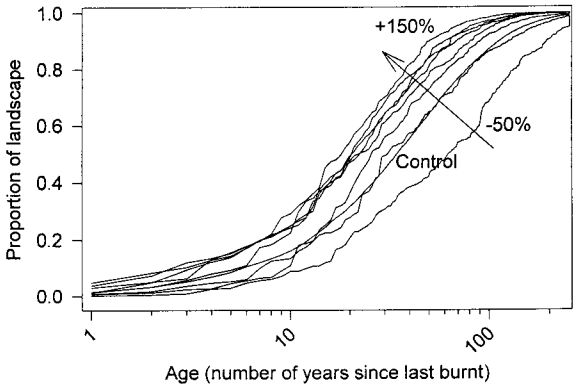

Figure 10. Cumulative age distribution of pixels in landscapes simulated according to varying rates of primary ignition events. Each line corresponds to the cumulative distribution of pixel ages in a landscape of 4 million pixels (160 km on a side) simulated with a different rate of primary ignition events, chosen to vary in 25% increments of the chosen control valve (0.00061 events per km^2/yr) from 50% less to 150% more. Note logarithmic x-axis.

way to produce reasonable looking fire size frequency distributions. Studies of experimental fire spread in this and other fuel types support this hypothesis (Burrows et al. 1991; Cheney et al. 1993; Cheney and Gould 1995). Our choice of a constant wind threshold independent of time since last fire and below which fire spread ceases is almost certainly unrealistic. This threshold is probably reduced or even eliminated in continuously distributed fuels (Gill et al. 1995). However while our choice of threshold (2 m/s ~ 7 km/h) is low compared to published suggestions (McArthur 1972; Burrows et al. 1991) it is close to that of Griffin and Allan (1984). It is best viewed as an average over different stand ages. Nonetheless, the critical role of wind variability in determining fire cessation remains only a hypothesis, and presence and spatial configuration of permanently unburnable elements in landscapes could play a fundamental role in determining fire size frequency distributions, particularly in landscapes in which fuel recovery times are longer.

Table 3. Patch statistics for landscapes simulated with different rates of 1° IEs.

Fire regime	0–4 yr Early			5–12 yr Mid			13–15 yr Late			26+ yr Mature			
	%[a]	#/km^2[b]	area[c] (km^2)	%	#/km^2	area (km^2)	%	km^2	area (km^2)	%[d]	%[e]	km^2[f]	area[g] (km^2)
1° IEs down 50%	2.6	0.002	16.64	7.2	0.003	20.3	16.5	0.0197	8.38	74.6	0.12	0.087	0.01
1° IEs down 25%	2.8	0.002	12.87	14.6	0.008	17.4	20.3	0.0403	5.03	62.9	1.15	0.155	0.07
Control	4.2	0.003	15.12	10.6	0.008	14.0	20.1	0.0319	6.36	65.1	0.03	0.168	0.02
1° IEs up 25%	4.7	0.004	13.18	12.8	0.012	10.4	30.4	0.0646	5.19	52.1	30.8	0.257	1.20
1° IEs up 50%	12.1	0.003	34.50	16.8	0.036	4.6	24.9	0.1145	2.18	48.1	21.6	0.283	0.76
1° IEs up 75%	8.1	0.007	12.35	25.5	0.012	21.5	23.2	0.1786	1.30	44.3	10.1	0.277	1.59
1° IEs up 100%	13.6	0.006	22.02	14.3	0.038	3.8	30.6	0.1436	2.12	43.1	7.9	0.277	0.25
1° IEs up 125%	12.9	0.007	19.71	14.9	0.029	5.0	34.8	0.1436	2.43	40.8	40.8	0.336	1.21
1° IEs up 150%	13.1	0.008	17.47	20.8	0.046	4.6	30.8	0.1977	1.56	36.8	36.8	0.355	1.04

[a]Percentage of the landscape of specified age, based on landscapes of 4 million pixels (25,600 km^2).
[b]Average number of patches of a specified age per km^2.
[c]Average area of patches of specified ages.
[d]Percentage of landscape 26 years and older, all patches.
[e]Percentage of landscape 26 years and older, excluding patches constituting >20% of total landscape. This renders the figures highly variable depending on the size of the dominant background patch and wether it is above or below the (arbitrary) 20% threshold.
[f]Average number of patches of a specified age per km^2, excluding patches constituting >20% of total landscape.
[g]Average area of patches of specified ages, excluding patches constituting >20% of total landscape.

The importance of unburnable elements in landscapes is hinted at by the fact that our simulation model resulted in fire scars with greater edge complexity than real fires. Addition of large simply shaped unburnable elements might result in simulated fire scars with simpler geometry closer to those recovered from the imagery.

We proceed by acknowledging that while our proposed model of fire spread is plausible, it is undoubtedly overly simplistic, but note that even if seriously in error, would not necessarily render our predictions regarding large scale dynamics and correlation structure of the landscape seriously flawed, given the reasonable fits of observed and simulated fire geometry statistics. The same is not true of predictions resulting from alternative fire burning regimes, which are clearly more sensitive to inaccuracies in the underlying process of fire occurrence and spread.

Simple analytic fire disturbance models predict that the cumulative distribution of elements in landscapes unburnt for T years, $C(T)$, will follow a Weibull distribution (Van Wagner 1978; Johnson and Wagner 1984, but see Reed et al. (1998) for more sophisticated models):

$$C(T) = \exp(-(T/b)^c). \quad (1)$$

Parameter c determines propensity of elements of different ages to burn, when $c = 1$, probability of burning is independent of age and Equation (1) reduces to a simpler exponential form. With $c > 1$, probability of burning increases with age. Parameter b has been termed fire recurrence time (Johnson 1979), and is the fire interval exceeded 37% of the time. Parameters b and c are easily recovered from data (Figure 2) using non-linear regression, and provide estimates of $b \sim 52$ yr (se: 0.12), and $c \sim 1.1$ (se 0.004).

Given rapid recovery time of vegetation following fire, and an average fire size of ~30 km^2, it is somewhat surprising to find evidence of correlation structure in the landscape at scales of hundreds of kilometers (see Figures 3 and 5): total areal extent of landscape dynamics appears to far exceed the size of their basic 'footprint'. Of course, to average out stochastic oscillations in these processes it would be prudent to maintain landscape units several times the dimensions of their correlation lengths. A lower estimate of the correlation length of the GVD landscape would be about 150 km, while evidence in Figure 5 suggests it may be twice this distance.

Temporal dynamics of habitat type at these correlation lengths indicates presence of vague low frequency cycles, which span larger (and higher) frequency ranges as younger habitat is considered. Spectral den-

sity analysis suggests that periods of these cycles may be as long as 200 years for older habitat, and as little as 10 for younger habitat. Given that these cycles emerge from models with stationary parameters (fire ignition is modelled as a Poisson process with constant mean), caution should be exercised in attributing apparent medium term trends to environmental change, even when observed on timescales of decades. On a similar note, natural variability in fire occurrence over time is considerable. The proportion of landscape composed of early successional habitat (0–4 years old) in a landscape window of over 6000 km^2, varied entirely naturally between 0.4% and 27.5%, suggesting that once again identifying real underlying change will be difficult. This result supports earlier work in different systems (e.g., Baker et al. 1991) in suggesting that landscapes have not yet been modelled at large enough spatial scales that fluctuations in these sort of large scale disturbance processes are 'averaged out'. Methods for determining appropriate spatial scale at which to study these processes remain embryonic (see Johnson and Gutsell (1991) for discussion).

Inspection of singular spectra of these time series suggests that this dynamical behavior emerges as a result of a largely stochastic process. Even when dynamics are viewed at spatial scales carefully chosen to maximize deterministic signal, such signal is largely undetectable or of very high dimensionality. No emergent low dimensional deterministic landscape dynamic appears to arise from this successionally driven fire cycle. Use of SVD for estimation of deterministic dimensionality has been questioned (see Palus and Dvorak 1992; Mees et al. 1987; Broomhead et al. 1988), like all forms of time series analysis, considerable caution should be exercised in its application and interpretation.

We have some confidence regarding predictions of large scale patch structure in this landscape, as they necessarily follow from accumulation of fire scars. However, small scale patch structure may be sensitive to exaggerated edge complexity of simulated fires. The conclusion that this landscape is composed of few large young patches, embedded in an essentially mature sea of surrounding habitat is unavoidable. Intermediate and late successional habitat must exist in more numerous patches somewhat smaller than the young habitat. Small patches of mature habitat are likely to be scattered throughout younger habitat. This patch structure is likely to impose somewhat different selection pressures on dispersal habits of species indigenous to each of these various patch types.

An important consequence of the assumptions of our simulations is that fire size frequency distributions are relatively insensitive to changes in fire frequency. Because vegetation recovers to a burnable state so fast following fire, and because fire duration is determined by meteorological conditions, changes in fire frequency have little impact on average fire size. Our simulations do predict that fires will spread faster in more mature habitat, but insensitivity of average fire size to changes in fire frequency is reflected by results suggesting that changing fire frequency by $\pm 50\%$ does not significantly modify average fire size.

Our model has prompted, sharpened and answered many questions regarding the temporal and spatial dynamics of fire driven habitat mosaics as they might occur in the Great Victoria Desert. None-the-less, we must emphasize that we have only analyzed output from a model, and what it tells us about these processes rests fully on the assumptions underlying the model's structure. Perhaps the most questionable of these assumptions is that the entire landscape is potentially burnable. We know that this is incorrect, but remain uncertain as to whether this renders the model's predictions seriously erroneous. Inclusion of unburnable elements could simply soften the relationship between fire spread and wind strength, and modify predicted fine scale patch structure. Alternatively, if might completely eliminate the need for temporal heterogeneity in fire spread probability, and totally transform our predictions regarding insensitivity of fire size to fire frequency. The study of the role of extent and configuration of unburnable elements in the landscape requires further study.

Acknowledgements

We are grateful to Alun Lloyd for much valuable assistance with the time series analysis. This study was funded by NASA, NSF and the Denton A. Cooley Centennial Professorship in Zoology, University of Texas, Austin.

Appendix 1

Wind strength probabilities (1500 h) – cumulative (conditional on strength greater than 5 m/s):

Wind Strength (m/s) (WS)	≥ 5 < 8	≥ 8 < 11	≥ 11
Probability	0.93	0.98	1.00

Wind direction probabilities (1500 h) – cumulative :

Wind direction (WD)	Probability	Wind direction (WD)	Probability
NE	0.053	SW	0.74
E	0.16	W	0.86
SE	0.39	NW	0.97
S	0.67	N	1.00

Wind change transition matrix, at 1500 h – cumulative (units meters per second):

From/To	WS < 2	WS ≥ 2 < 5	WS ≥ 5 < 8	WS ≥ 8 < 11	WS ≥ 11
WS < 2	0.40	0.89	0.97	0.99	1.00
WS ≥ 2 < 5	0.23	0.81	0.93	0.98	1.00
WS ≥ 5 < 8	0.15	0.60	0.87	0.97	1.00
WS ≥ 8 < 11	0.11	0.53	0.77	0.94	1.00
WS ≥ 11	0.15	0.57	0.70	0.83	1.00

WS = wind strength.

Wind change transition matrix, from 0900 h – cumulative (units meters per second):

From/To	WS < 2	WS ≥ 2 < 5	WS ≥ 5 < 8	WS ≥ 8 < 11	WS ≥ 11
WS < 2	0.57	0.93	0.98	0.99	1.00
WS ≥ 2 < 5	0.30	0.87	0.95	0.98	1.00
WS ≥ 5 < 8	0.14	0.62	0.88	0.97	1.00
WS ≥ 8 < 11	0.07	0.45	0.73	0.92	1.00
WS ≥ 11	0.08	0.32	0.49	0.75	1.00

WS = wind strength.

Appendix 2. Algorithm for fire ignition and spread

The algorithm starts with a single burning pixel resulting from a 1° IE. The annual number of fires that spread over more than 4 pixels (G) is modelled as a Poisson variable with mean γn^2 (where γ is density of observed fires >4 pixels in size per pixel per year, and n^2 is the number of pixels in the lattice). γ was estimated to be 3.9×10^{-6} per pixel per year (Haydon et al. 1999). Primary ignition events are initiated sequentially until G fires (all >4 pixels) result. Time within a year and seasonality are not explicitly recorded. Because most wildfires in this region are ignited by lightning, we assumed that 1° IEs occurred at a designated start time selected with uniform probability from between 1500 and 0100 (reflective of the timing of 1° IEs reported by Nash and Johnson (1996) – albeit for a different location), at which point wind direction and strength are assigned from one of 8 and 5 categories respectively based on probability distributions derived from observed frequencies of wind direction and strength, (conditional on strength of at least 5 m/s). Wind direction is assumed to remain constant throughout the burn.

2° IEs are initiated immediately subsequent to a primary ignition event. Each ignited pixel is permitted N opportunities (trials) to ignite each of its 8 neighboring non-burning neighbors after which the pixel is deemed to have burned out. Each trial is assumed to represent a fixed length of time t (hours), each pixel therefore burns for a fixed time interval given by the product Nt (in our model parameters were selected that allowed this product to vary between 4 and 13 h). Both N and t are independent of pixel age.

Probability that fire spreads to any of its neighboring non-burning pixels at each trial is independent of age of the burning pixel, but increases with age of the non-burning pixel, current wind strength, a tuning parameter (F) and direction of the neighboring non-burning pixel from the burning pixel relative to current wind direction. Degree of bias introduced by wind direction is determined by parameter k_b. The probability that any one of these trials is successful, and that fire spreads to a previously non-burning pixel is given by the product:

$$P[2°\text{IE}] = S_{\text{wind\_strength}} \times A'_{\text{age}} \times B_{\text{wind\_bias}} \times F$$

(see below for definition of terms). Realization of the occurrence of 2°IEs is determined using these proba-

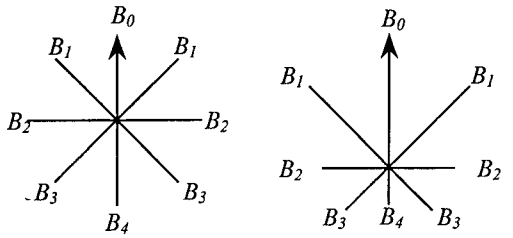

Figure A1 Bias factors, (A) no wind, (B) wind blowing as indicated.

bilities and a random number generator. Pixels either burn or not, and ignite only once.

The subscript wind_strength refers to which of the 5 categories of current wind strength currently assumed, the S vector was assumed to be = [0, 0.5, 0.75, 1.0, 1.0]. Thus when wind dropped below 2 m/s 2° IEs cease, but 2° IEs became progressively more likely with increasing wind strength.

Probability of fires spreading to pixels of differing age classes was investigated in the preceding paper (Haydon et al. 1999). We fitted a Weibull distribution to these data, obtaining the following predictive equation:

$$P[\text{fire spread to pixel of age } x] = 1 - \exp(-0.76x)^{0.23}$$

A_{age} was set equal to P[fire spread to pixel of age x] for $x > 3$, $A[1]$, $A[2]$ and $A[3]$ were set equal to zero, thereby eliminating any probability that fire could spread to pixels that had burned in the last 3 years. However these empirical probabilities are clearly the final result of a series of N 2° IEs, and what is required is the *per trial* probability of spread A'_{age}. If there are to be N such trials, the probability of spread at each trial can be shown to be $A'_{\text{age}} = 1 - \exp\left(\ln(1 - A_{\text{age}})/N\right)$. A_{age}, P[fire spread to pixel of age x] and empirical data are shown in Figure 1B.

The B vector corresponds to wind bias. The *bias* subscript refers to one of 5 different directions that the non-burning pixel might lie in relative to the burning pixel and current wind direction. When $bias = 0$ the alignment corresponds to the situation in which the non-burning pixel lies directly downwind from the burning pixel, $bias = 4$ to when the non-burning pixel lies directly upwind from the burning pixel, and so on, as shown in Figure A1.

$$B_4 = 0.125 \cdot q,$$
$$B_3 = [0.125 + 0.125 \cdot 0.5 \cdot (1 - q)]q,$$
$$B_2 = [0.125 + [0.125 + 0.125 \cdot 0.5 \cdot (1 - q)](1 - q)]q,$$
$$B_1 = [0.125 + [0.125 + [0.125 + 0.125 \cdot 0.5 \cdot (1 - q)](1 - q)](1 - q)]q,$$
$$B_0 = 0.125 + 2[0.125 + [0.125 + [0.125 + 0.125 \cdot 0.5 \cdot (1 - q)](1 - q)](1 - q)](1 - q)$$

and

$$q = \exp(-k_b \cdot W_{\text{wind\_strength}}).$$

$W_{\text{wind\_strength}}$ is a vector containing a measure of wind speed (in m/s) for each of the 5 wind speed categories. $W = [1, 4, 7, 10, 13]$. This is simply a way of re-distributing probability in different directions (note that $B_4 + 2B_3 + 2B_2 + 2B_1 + B_0 = 1$), according to current wind strengths and directions. The parameter k_b determines sensitivity of bias in fire spread direction to wind strength (large values of k_b correspond to high levels of bias for a given wind strength.

Parameter F can be used to vary probability of 2° IEs without introducing differential spread with regard to wind patterns or pixel age.

Fires spread by effectively performing simultaneous mass trials testing for the occurrence of 2° IEs between all neighboring burning and non-burning pixels. After each round of trials, time is updated by t, and pixels that have undergone N trials are 'extinguished'. If time passes over 0900 or 1500 wind strength is re-determined from the appropriate wind strength transition matrix. Fires burn out when all burning pixels associated with a single 1° IE have been extinguished. Fires burn one at a time on the landscape, no other 1° IEs are initiated until the probability of further 2° IEs associated with the previous 1° IE is zero. After G fires have been burned, various structural attributes of the landscape are computed, and age of all pixels in the landscape incremented by 1 year.

Appendix 3.

Parameters in bold on the first row represented the 'center' of the sensitivity analysis, and the goodness-of fit was not bettered by any other combination of parameter choices so were selected in simulation of 'control' landscapes.

Best 10 parameter combinations from the 82 combinations that constituted the sensitivity analysis.

N	k_b	t	F	χ^2_A	χ^2_P	χ^2_{ES}	χ^2_{MM}	χ^2_0	χ^2_0 omitting χ^2_{ES}
50	**0.4**	**0.15**	**2.6**	155	182	396	244	523	341
65	0.52	0.195	2.6	105	214	439	155	523	284
50	0.4	0.195	1.82	154	187	400	233	523	336
65	0.4	0.15	1.82	125	175	387	297	533	366
65	0.52	0.15	2.6	188	250	428	171	557	356
65	0.4	0.195	1.82	208	195	402	271	563	393
50	0.4	0.195	2.6	126	187	408	327	570	397
65	0.4	0.105	1.82	109	147	524	140	573	230
35	0.4	0.195	3.38	190	286	443	181	589	388
50	0.52	0.195	3.38	114	287	461	216	596	376

References

Antonovski, M.Y., Ter-Mikaelian, M.T. and Furyaev, V.V. 1992. A spatial model of long term forest fire dynamics and its applications to forests in Western Siberia. Pp. 373–403. *In* A systems Analysis of the Global Boreal Forest. Edited by Shugart, H.H., Leemans, R. and Bonan, G.B. Cambridge University Press, Cambridge.

Abarbanel, H.D.I., Brown, R., Sodorowich, J.J. and Tsimring, L.S. 1993. The analysis of observed and chaotic data in physical systems. Rev. Modern Phys. 65: 1331–1393.

Baker, W.L., Egbert, S.L. and Frazier, G.F. 1991. A spatial model for studying the effects of climatic change on the structure of landscapes subject to large disturbances. Ecol Model 56: 109–125.

Baker, W.L. 1993. Spatially heterogenous multi-scale response of landscapes to fire suppression. Oikos 66: 6–71.

Baker, W.L. 1994. Restoration of landscape structure altered by fire suppression. Conserv Biol 8: 763–769.

Boychuk, D., Perera, A.H., Ter Mikaelian, M., Martell, D.L and Li, C. 1997. Modelling the effect of spatial scale and correlated fire disturbances on forest age distribution. Ecol Model 95: 145–164.

Bradstock, R.A. and Gill, A.M. 1993. Fire in semi-arid Mallee shrublands: size of flames from discrete fuel arrays and their role in the spread of fire. Int J Wildland Fire 3: 3–12.

Bradstock, R.A., Bedward, M., Scott, J. and Keith, D.A. 1996. Simulation of the effect of spatial and temporal variation in fire regimes on the population viability of a *Banksia* species. Conserv Biol 10: 776–784.

Broomhead, D.S. and King, G.P. 1986. Extracting qualitative dynamics from experimental data. Physica 20D: 217–236.

Broomhead, D.S., Jones, R. and King, G.P. 1988. Comment on 'Singular-value decomposition and embedding dimension'. Phys Rev A37: 5004–5005.

Burrows, N., Ward, B. and Robinson, A. 1991. Fire behaviour in spinifex fuels on the Gibson Desert Nature Reserve, Western Australia. J Arid Environ 20: 189–204.

Chatfield, C. 1996. The analysis of times series: an introduction. Chapman and Hall, New York.

Cheney, N.P., Gould, J.S. and Catchpole, W.R. 1993. The influence of fuel, weather and fire shape variables on fire spread in grasslands. Int J Wildland Fire 3: 31–44.

Cheney, N.P. and Gould, J.S. 1995. Fire growth in grassland fuels. Int J Wildland Fire 5: 237–247.

Davis, F.W. 1993. Introduction to spatial statistics. Pp. 16–26. *In* Patch Dynamics. Edited by Levin, S.A., Powell, T.M. and Steele, J.H. Springer-Verlag, Berlin.

Gardner, R.H., Hargrove, W.W., Turner, M.G. and Romme, W.H. 1996. Global change disturbances and landscape dynamics. Pp. 149–172. *In* Global change and terrestrial ecosystems. Edited by Walker, B. and Steffen, W. Cambridge University Press, Cambridge.

Gill, A.M., Burrows, N.D. and Bradstock, R.A. 1995. Fire modelling and fire weather in an Australian desert. CALMScience Suppl 4: 29–34.

Gill, A.M. and Williams, J.E. 1996. Fire regimes and biodiversity – the effects of fragmentation of southeastern Australian eucalypt forests by urbanization, agriculture and pine plantations. For Ecol Manage 85: 261–278.

Green, D.G. 1989. Simulated effects of fire, dispersal and spatial pattern on competition within forest mosaics. Vegetatio 82: 139–153.

Griffin, G.F., Price, N.F. and Portlock, H.F. 1983. Wildfires in the central Australian rangelands 1970–1980. J Environ Manage 17: 311–323.

Griffin, G.F. and Allan, G.E. 1984. Fire behaviour. Pp. 55–68. *In* Anticipating the Inevitable: a Patch Burn Strategy for Fire Management at Uluru (Ayers Rock-Mt Olga) National Park. Edited by Saxon, E. CSIRO Australia, Melbourne.

Griffin, G.F., Morton, S.R. and Allan, G.E. 1988. Fire-created patch- dynamics for conservation management in the hummock grasslands of central Australia. Proc. International Grasslands Symposium, Huhhot, China.

Hansson, L., Fahrig, L. and Merriam, G. (eds). 1995. Mosaic landscapes and ecological processes. Chapman and Hall, London.

Haydon, D.T., Friar, J. and Pianka, E.R. 1999. Fire Driven Dynamic habitat mosaics in the Great Victoria Desert: I. Fire Geometry. Landscape Ecol 14: 373–381.

Huston, M.A. 1996. Biological Diversity: The Coexistence of Species on Changing Landscapes. Cambridge University Press, Cambridge.

Isham, V. 1991. Assessing the variability of stochastic epidemics. Math Biosci 107: 209–224.

Iwasa, Y. and Kubo, T. 1995. Forest gap dynamics and partially synchronized disturbances and patch age distribution. Ecol Model 77: 257–271.

Johnson, E.A. 1979. Fire recurrence in the subarctic and its implications for vegetation composition. Can J Bot 57: 1374–1379.

Johnson, E.A. 1991. Fire and Vegetation Dynamics. Studies from the North American Boreal Forest. Cambridge Studies in Ecology. Cambridge University Press, Cambridge.

Johnson, E.A. and Gutsell, S.L. 1991. Fire frequency models, methods and interpretations. Adv Ecol Res 25: 239–287.

Johnson, E.A. and Van Wagner, C.E. 1984. The theory and use of two fire history models. Can J For Res 15: 214–220.

Kendall, D.G. 1956. Deterministic and stochastic epidemics in closed populations. Proc Third Berkeley Symp Math. Statist and Prob 4: 149–165.

Kimber, R. 1983. Back lightning: Aborigines and fire in central Australia and the Western Desert. Archeology in Oceania 18: 38–45.

Li, C. and Apps, M.J. 1996. Effects of contagious disturbance on forest temporal dynamics. Ecol Model 87: 143–151.

Li, C., Ter Mikaelian, M. and Perera, A. 1997. Temporal disturbance patterns on a forest landscape. Ecol Model 99: 137–150.

Lindenmayer, D.B. and Possingham, H.P. 1995. Modelling the impacts of wildfire on the viability of metapopulations of the endangered Australian species of arboreal marsupial, Leadbeaters possum. For Ecol Manage 74: 197–222.

McArthur, A.G. 1972. Fire control in arid and semi-arid lands of Australia. *In* The Use of Trees and Shrubs in the Dry Country of Australia. Edited by N. Hall et al. Australian Government Publishing Service, Canberra.

Mckenzie, D., Peterson, D.L. and Alvarado, E. 1996. Extrapolation problems in modelling fire effects at large spatial scales: a review. Int J Wildland Fire 6: 165–176.

Mees, A.I., Rapp, P.E. and Jennings, L.S. 1987. Singular-value decomposition and embedding dimension. Phys Rev A36: 340–341.

Minnich, R.A. and Chou, Y.H. 1997. Wildland fire patch dynamics in the chaparral of southern California and Northern Baja California. Int J Wildland Fire 7: 221–248.

Moloney, K.A. and Levin, S.A. 1996. The effects of disturbance architecture on landscape-level population dynamics. Ecology 77: 375–394.

Morton, S.R., Smith, D.M.S., Friedel, M.H., Griffin, G.F. and Pickup, G. 1995. The stewardship of arid Australia: ecology and landscape management. J Environ Manage 43: 195–217.

Nash, C.H. and Johnson, E.A. 1996. Synoptic climatology of lightening-caused forest fires in subalpine and boreal forests. Can J For Res 26: 1859–1874.

O'Neill, R.V., Gardner, R.H., Turner, M.G. and Romme, W.H. 1992. Epidemiology theory and disturbance spread on landscapes. Landscape Ecol 7: 19–26.

Paine, R.T. and Levin, S.A. 1981. Intertidal landscape:disturbance and the dynamics of pattern. Ecol Monogr 51: 145–178.

Palus, M and Dvorak, I. 1992. Singular-value decomposition in attractor reconstructions: pitfalls and precautions. Physica D55: 221–234.

Pianka, E.R. 1996. Long-term changes in lizard assemblages in the Great Victoria desert: Dynamic habitat mosaics in response towildfires. Pp. 191–21. *In* Long-Term Studies of Vertebrate Communities. Edited by Cody, M.L. and Smallwood, J.A. Chapter 8, Academic Press, New York.

Pickett, S.T.A. and White, P.S. 1985. The ecology of natural disturbance and patch dynamics. Academic Press, New York.

Rand, D.A. and Wilson, H.B. 1995. Using spatio-temporal chaos and intermediate-scale determinism to quantify spatially extended ecosystems. Proc R Soc Lond Ser B Biol Sci 259: 111–117.

Ratz, A. 1995. Long-term spatial patterns created by fire: A model oriented towards boreal forest. Int J Wildland Fire 5: 25–34.

Reed, W.J., Larsen, C.P.S., Johnson, E.A. and MacDonald, G.M. 1998. Estimation of temporal variations in historical fire frequency from time since fire map data. For Sci 44: 465–475.

Romme, W.H. 1982. Fire and landscape diversity in subalpine forests of Yellowstone National Park. Ecol Monogr 52: 199–221.

Russellsmith, J., Ryan, P.G. and Durieu, R. 1997. A landsat MSS-derived fire history of Kakadu National Park, monsoonal northern Australia, 1980–94 – seasonal extent, frequency and patchiness. J Appl Ecol 34: 748–766.

Schimmel, J. and Granstrom, A. 1997. Fuel succession and fire behavior in the Sedish boreal forest. Can J For Res 27: 1207–1216.

Stauffer, D. and Aharony, A. 1992. Introduction to percolation theory. Taylor and Francis, New York.

Taylor, D.L. 1973. Some ecological implications of fire control in Yellowstone National Park. Ecology 54: 1394–1396.

Turner M.G., Romme, W.H. and Gardner, H. 1994a. Landscape disturbance models and the long-term dynamics of natural areas. Nat Areas J 14: 3–11.

Turner M.G., Hargrove, W.W., Gardner, R.H. and Romme, W.H. 1994b. Effects of fire on landscape heterogeneity in Yellowstone National Park, Wyoming. J Veg Sci 5: 731–742.

Turner M.G., Romme, W.H., Gardner, R.H. and Hargrove, W.W. 1997. Effects of fire size and pattern on early succession in Yellowstone National Park. Ecol Monogr 67: 411–433.

Van Wagner, C.E. 1978. Age-class distribution and the forest fire cycle. Can J For Res 8: 220–227.

Wallin, D.O., Swanson, F.J., Marks, B., Cissel, J.H. and Kertis, J. 1996. Comparison of managed and pre-settlement landscape dynamics in forests of the Pacific Northwest USA. For Ecol Manage 85: 291–309.

Wu, Y., Sklar, F.H., Gopu, K. and Rutchey, K. 1996. Fire simulations in the Everglades landscape using parallel programming. Ecol Model 93: 113–124.